December 2009 *Volume 3 Issue 2*

Trade Science Inc.

Nano Science and Nano Technology
An Indian Journal

Full Paper

NSNTAIJ, 3(2), 2009 [32-38]

Oxidative decomposition of malathion-pesticide by using manganese-doped Bi-Sr-vanadate nano-surface catalyst

M.Khaled Elsabawy[1#]*, M.Mosrsy Abou Sekkina[1], A.Mohamed Asker[1]
[1]Chemistry Department, Faculty of Science, Tanta University, Tanta-31725, (EGYPT)
[#]Chemistry Department, Faculty of Science, Materials Science Unit, Taif University, 888-Alhawya-Taif City-Kingdom of Saudi Arabia, (SAUDI ARABIA)
E-mail : ksabawy@yahoo.com; ksabawy@hotmail.com

Received: 13th December, 2009 ; Accepted: 23rd December, 2009

ABSTRACT

The kinetics of oxidative decomposition of malathion pesticide using selected manganese-doped Bi-Sr-Vanadate $Bi_2SrV_{1.9}Mn_{0.1}O_9$ was studied carefully in ethanolic solution in the presence of H_2O_2 under condition of pseudo-first order reaction. The catalyst was prepared by conventional solid state reaction technique; the structural and micro-structural properties of the catalyst were characterized well by XRD and SEM respectively. Many of the kinetic parameters were investigated in this article, results obtained indicated that, the rate of oxidative degradation of malathion was found to be pH-dependent. The mechanism was proposed and the activation parameters were calculated.

KEYWORDS

Manganese-doped vanadate;
Kinetics; SE-microscopy;
X-ray Diffraction;
Oxidative degradation;
Malathion.

INTRODUCTION

Technical malathion and many other pesticides constitute one of the largest groups of organophpsphorous compounds that represent an increasing environmental danger[1,2]. One of the novel technologies for treating polluted water and wastewater is the advanced oxidation processes (AOPs), by which hydroxyl radicals (·OH) are generated to degrade organic pollutants[3].

Throughout the 20th century, the mechanisms, kinetics, and products of the AOPs using hydrogen peroxide (H_2O_2), ozone (O_3), UV or ultrasonic irradiation, titanium dioxide (TiO_2), and Fenton's reagent, which is a combination of ferrous ions and H_2O_2, were investigated extensively. These treatments were studied separately or in various combinations[4-7].

Technical malathion and their formulation types have a broad spectrum insecticidal control of sucking and chewing insects, including aphids, house flies, mosquitoes, scale insects and spider mites. Used in fruits, ornamentals, beans, vegetables, and stored products. It can be applied on the same day as grazining or harvesting. Malathion have acute oral LD50 for rate 1375mg\kg, mice 775mg\kg, cattle 500mg\kg, rabbite 4100mg\kg. Also it toxic to bees and fish[8].

J.Wang et al.[9] confirm that nanometer rutile titanium oxide powder TiO_2 can be used as sonocatalytic degradation of organic pollutants for treating organic waste water.

The essential goal of present article is describing a new trend for application of Mn-doped Bi-Sr-vanadate ceramic as an active surface catalyst for oxidative degradation of technical malthion pesticide.

EXPERIMENTAL

Preparations

Catalyst synthesis

The Mn-doped samples with general formula $Bi_2SrV_{2-x}Mn_xO_9$ where x = 0.1 mole were prepared by conventional solid state reaction route and sintering procedure using appropriate amount of $Bi_2(CO_3)_3$, $SrCO_3$, $(NH_4)_2VO_3$ and $MnCO_3$ each purity >99%. The mixture was ground in an agate mortar for one hour. Then the finely ground powder was subject to firing at 800°C for 10 hours and reground and finally pressed into pellets with thickness 0.2cm and diameter 1.2cm. Sintering process was carried out at 850°C for 10 hours. Then the furnace is cooled slowly down to room temperature. Finally the materials are kept in vacuum desiccator over silica gel dryer.

Malathion source and solutions

Technical malathion (Chimenova) was supplied from Kafr Elzayat for Pesticides and Chemicals Co., figure (1) It was characterized by gas chromatography [Perkin El-mer] figure (2) and carefully spectrophotometrically at $\lambda_{max.}$ 420nm[8].

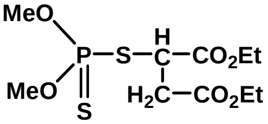

Figure 1 : The structure of technical malathion.

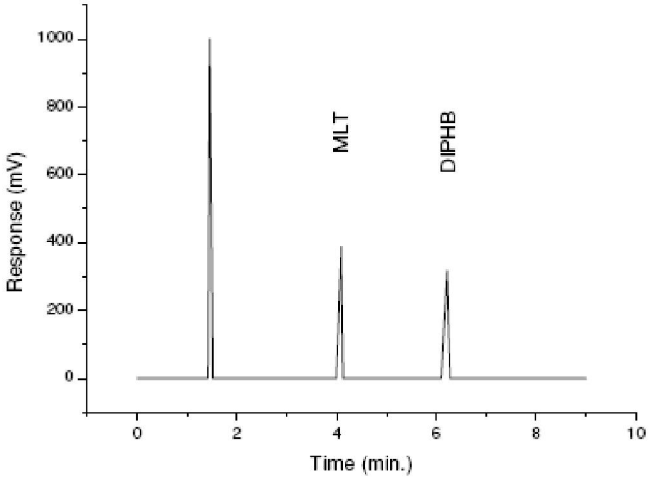

Figure 2 : Gas chromatogram for technical malathion.

Catalyst characterization

X-ray diffraction (XRD)

The X-ray diffraction measurements (XRD) were carried out at room temperature on the fine ground $Bi_2SrV_{1.9}Mn_{0.1}O_9$ systems on the range (2θ=10-70°) using Cu-Kα radiation source and a computerized [Bruker Axs-D8 advance] X-ray diffractometer with two theta scan technique. Analysis of the corresponding 2θ values and the interplanar spacing d (A°) by using computerized program proved that the compound is mainly belongs to distorted perovskite type with hexagonal crystal form, that expressed by assigned peaks figure (3). The unite cell dimensions were calculated using parameters of the most intense x-ray reflection peaks.

Scaning electron-microscope (SEM)

Scaning electron microscope (SEM) measurements were carried out using small pieces of prepared samples on different sectors to be the actual molar ratios by using "TXA-840, JEOL-Japan" attached to XL30 apparatus with EDX unit, accelerant voltage 30kv, magnification 10x up to 500.000x and resolution 3nm. The samples were coated with gold. Figure (4) show the SEM of the catalyst surface. The average grain size

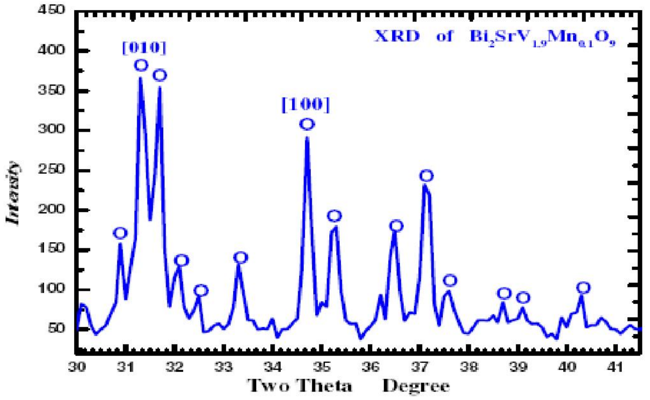

Figure 3 : The X-ray diffraction pattern for $Bi_2SrV_{1.9}Mn_{0.1}O_9$ regime.

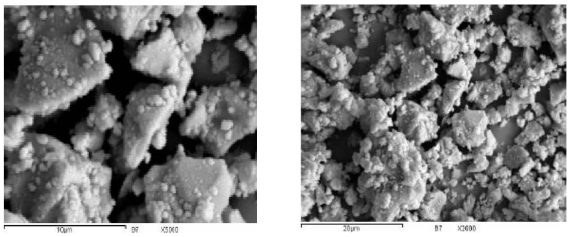

Figure ($4_{a,c,e}$) : SE-micrographs images recorded for $Bi_2SrV_{1.9}Mn_{0.1}O_9$.

was calculated and found to be 2.49μm with estimated average particle size ranged in between 20-25nm.

Kinetic measurements

The kinetic measurements of the reaction were carried out using UV-VIS spectronic 601 spectrophotometer at $\lambda_{max.}$ 420nm for technical malathion.

RESULTS & DISCUSSION

Mechanism and order of reaction

The mechanism of oxidative degradation of technical malathion was proposed in our investigations as two step process. The first step, is the fast one which includes the reaction between hydrogen peroxide and Mn doped Bi-Sr-vanadate solid surface irreversibly with a rate constant K_1 (Eq. 1) to form intermediate activated complex C*, but this step is the fast one and irreversible.

The second step is the rate-determining step (slow step) includes the reaction between activated complex C* with the technical malathion with a rate constant K_2 (Eq.2).

$$H_2O_2 + [Bi_2SrV_{1.9}Mn_{0.1}O_9] \xrightarrow{K_1} [C^*] \quad (1)$$

$$[C^*] + [Dye] \xrightarrow{K_2} [P] + [Bi_2SrV_{1.9}Mn_{0.1}O_9] \quad (2)$$

Where [P] is decoloured oxidative malathion.

The mechanistic sequences may describes as follow: the addition of H_2O_2 to the catalyst ($Bi_2SrV_{1.9}Mn_{0.1}O_9$ surface) which includes different oxidation states of different ions but generally we will use symbol M^{+n} which indicate to all positive cations on the catalyst surface (Sr^{2+}, Bi^{2+}, Mn^{2+} and V^{5+}) which reacts with H_2O_2 forming μ^2 bound peroxide, which stabilized by hydrogen bonding[10-11] forming activated complex[C*] that finally reacts rapidly reversibly with substrate malathion oxidizing it as described in equation (2).

Robbins et al.[10] studied the activation of hydrogen peroxide for oxidation of quinaldine blue indicator by using copper ^{22} complexes and they reported that, using of metal redox mechanisms[12] for activation of H_2O_2 decomposition but, in their mechanism of activation H_2O_2 coordinates fastly with copper ^{22} with out any change in its oxidation state.

Order of the reaction

The order of reaction is evaluated by application the conditions of pseudo-first order reaction by keeping H_2O_2 in large excess and consequently, the overall reaction can be expressed as shows in Eq.(3).

$$[H_2O_2] + [Bi_2SrV_{1.9}Mn_{0.1}O_9] + [malathion] \xrightarrow{K_{true}} [Oxidized\ malathion] \quad (3)$$

Hence the rate of oxidation depends only on the concentration of malathion and can be expressed as follows:

$$Rate = K_{true}[H_2O_2][Bi_2SrV_{1.9}Mn_{0.1}O_9][malathion] \quad (4)$$

Where K_{true} is the true rate constant but,
$[Bi_2SrV_{1.9}Mn_{0.1}O_9]$ and $[H_2O_2] >>> [malathion]$
Thus, rate = $K_{obs.}$[malathion], where

$$K_{obs.} = K_{true}[H_2O_2][Bi_2SrV_{1.9}Mn_{0.1}O_9] \quad (5)$$

According to the first order reaction condition a plot between $\ln(A_t\text{-}A_o)$ and time was constructed giving straight lines (Figure $5_{a,b}$) with slop equal to observed rate constant $K_{obs.}$ and hence, the true rate constant K_{true} can be easily evaluated by knowing[catalyst] and $[H_2O_2]$. In this respect, A_t and A_o are the absorbance of the malathion at time t and infinity, respectively.

Malathion concentration effect

Figure ($6_{a,b}$) show the relation between the concentration of malathion and H_2O_2 respectively with the evaluated rate constant ($K_{obs.}$) and it is found that, the values of rate constant increase with increasing both of malathion concentration and hydrogen peroxide confirming that the oxidative degradation of malathion is a first order reaction under these conditions and hydrogen peroxide dependent.

According to Eq.1 and Eq.2, both of H_2O_2 and malathion play an important role in the reaction sequence since the hydrogen peroxide initially attacks the active centers on the catalyst surface forming μ^2 bound peroxide, which stabilized by hydrogen bonding[10-11] forming activated complex [C*] that finally reacts rapidly and reversibly with substrate malathion oxidizing it as described in equation (2). And by the same the increasing in the substrate malathion concentration must leads to correspondence increase in the reaction rates.

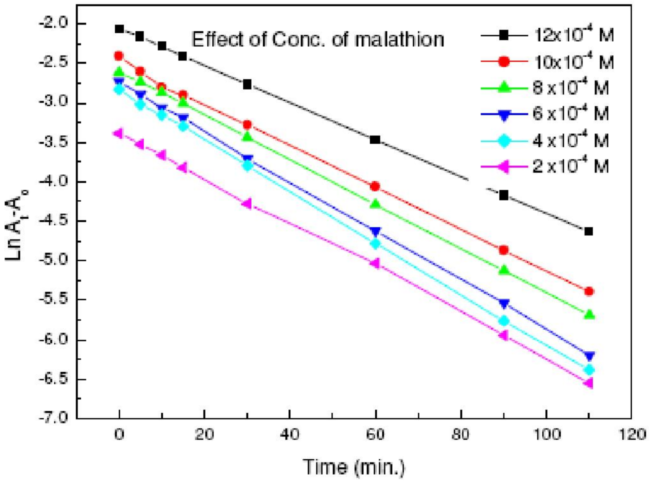

Figure(5a) : The first oxidative reaction of malathion different concentrations with wt.of catalysis = 0.02g, in the presence of H_2O_2 = 0.05M, Temp. 30°C and pH = 7.

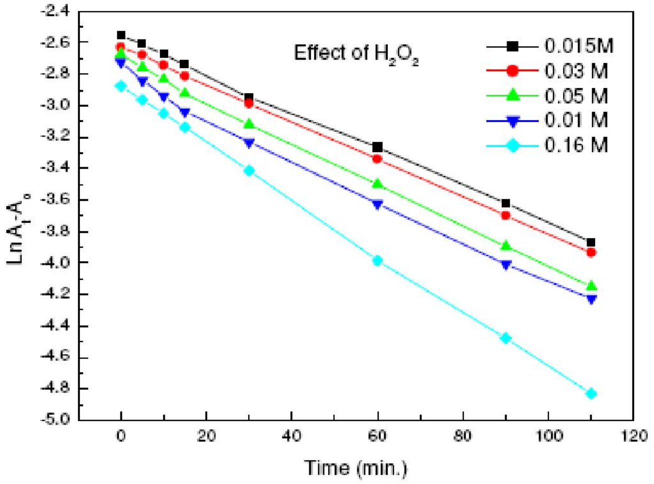

Figure(5b) :The first oxidative reaction of malathion 6×10^{-4} with wt.of catalysis = 0.02 g, Temp. 30°C, and pH = 7at different concentrations of H_2O_2.

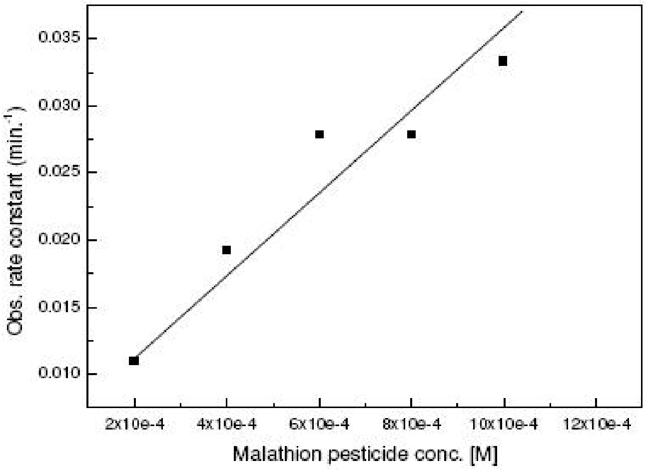

Figure(6_a) : The variation of observed rate constant ($K_{obs.}$) versus malathion concentrations.

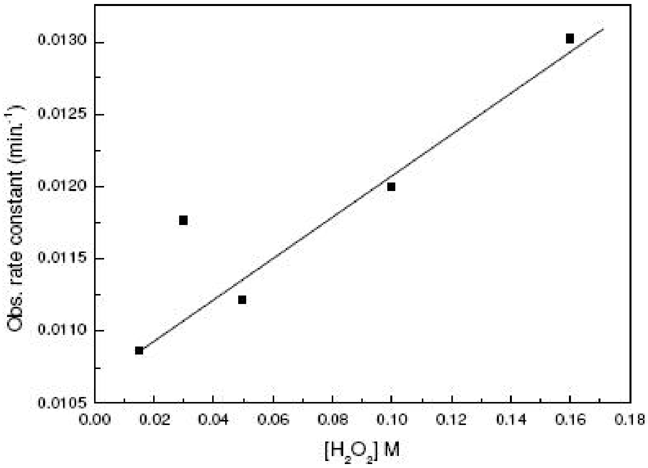

Figure(6_b) : The variation of observed rate constant ($K_{obs.}$) versus H_2O_2 concentrations.

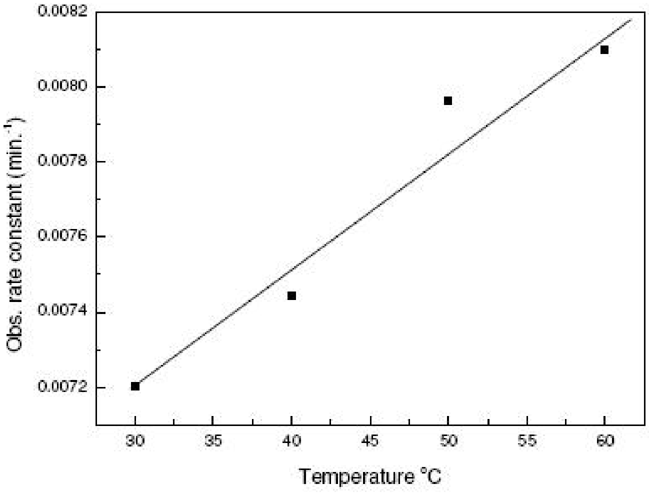

Figure(7) : The variation of observed rate constant ($K_{obs.}$) versus temperatures.

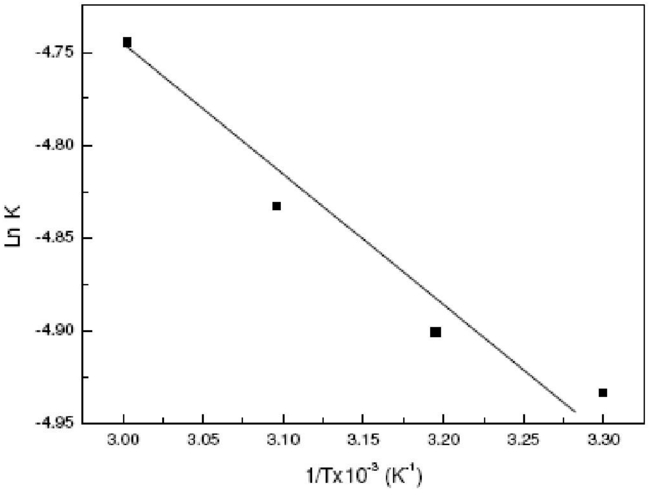

Figure(8) : Arrhenius plot for oxidative decomposition of malathion with Mn doped Bi-Sr-vanadate.

Temperature effect

Figure (7) display the effect of temperature on the reaction rate of degradation of the malathion. The reaction between [malathion] = 6×10^{-4}M with 0.02g of the catalyst at pH = 7 and H_2O_2 = 0.05 M was carried out at different temperatures.

It is found that, the rate of oxidative degradation of malathion with Mn-doped Bi-Sr-vanadate catalyst increases with increasing the temperature. It clear that the increasing of temperature causes an activation to the surface area of the Mn-doped Bi-Sr-vanadate catalyst that already reacted to reform new one and consequently the numbers of active centers will be raised yielding to correspondence increase on the reaction rate degradation process.

Determination of the activation parameters

Figure (8) displays the Arrhenius plot of lnK versus 1/T, where T is the absolute temperature K is the observed reaction rate constant at this temperature in accordance with the Eyring-Polanyi equation[13].

$$\mathbf{K = k_bT/h.e^{\Delta G^*/RT}} \qquad (6)$$

Where k_b and h are the Boltzmann's and Plank's constants, respectively.

From this plot, the activation energy was found E^*= 64.23 kJ/mole while the thermodynamics papameters of activation were found to be ΔH^* = 61.43 kJ/mol & ΔG^* = 81.17 KJ/mol and ΔS^* = -113.73 J/deg./mol respectively.

These thermodynamic activation parameters help to understand and support the proposed catalytic oxidative mechanism enhancing us to estimate how much the ease of such these reaction to occur spontaneously.

Buffer effect

The oxidative degradation of malathion was carried out at different pH-values using universal buffer. Figure (9) display that, the rate of oxidative degradation of malathion increases in the acidic medium ranged [pH = 2.5-4.5], alkaline medium [pH = 8,10] and decrease in neutral medium pH = 6.5[8].

These results are similar to those reported by Khaled M.Elsabawy et al.[14] due to the hydro peroxide anion $[HO_2]^-$ species is maximum in alkaline medium and consequently from the mechanistic proposal pathway, the formation of activated complex [C*] is maximum in alkaline medium. This means that the rate of oxidation for

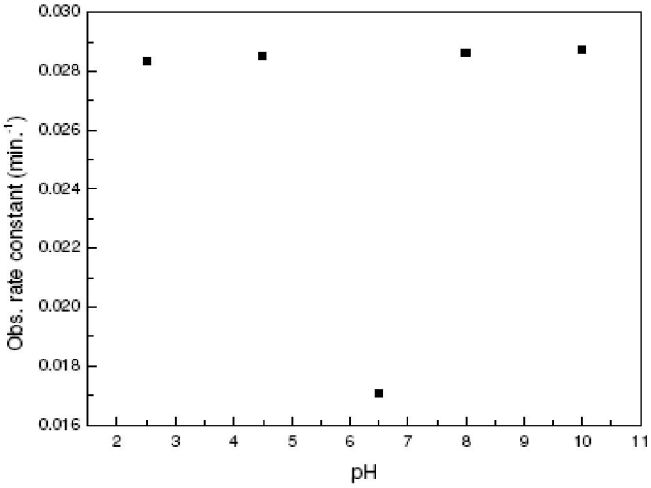

Figure(9) : The variation of observed rate constant ($K_{obs.}$) versus pH.

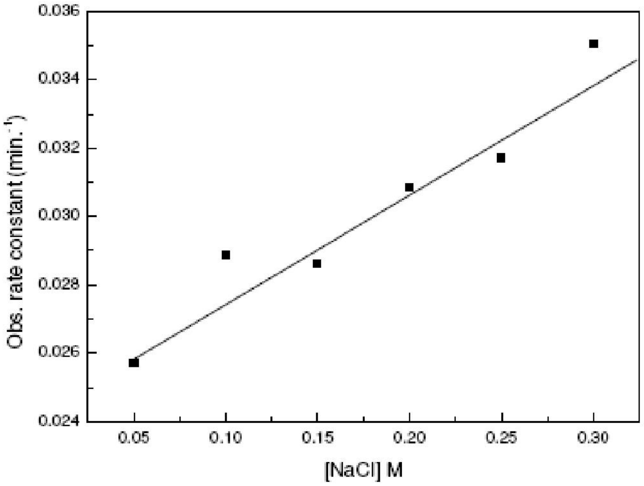

Figure (10_a) : The variation of observed rate constant ($K_{obs.}$) versus conc. of NaCl.

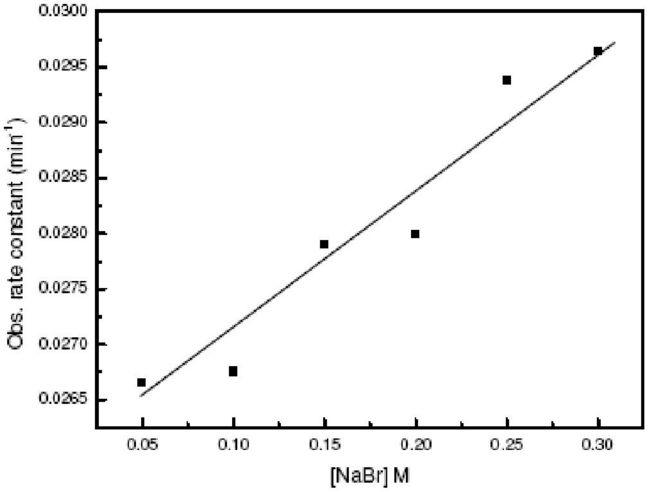

Figure (10_a) : The variation of observed rate constant ($K_{obs.}$) versus conc. of NaBr.

malathoin depend on pH and the oxidation efficiency on Mn-doped Bi-Sr-vanadate surface catalyst is maximum in acidic and alkaline medium.

Salt effect

Figure ($10_{a,b}$) show the effect of the [NaCl] and [NaBr] on the oxidation reaction rate of malathion. It is clear that, the increasing of salt concentration leads to an increase in the total ionic strength in the reaction medium and consequently increasing the adsorption of the substrate on the catalyst surface.

These results are in agreement with number of articles like[15-31] in which the kinetics investigations on the degradation of hazardous materials organic substrates were performed in presence of hydrogen peroxide and metal oxide surface catalyst.

CONCLUSION

The kinetics of oxidative decomposition of malathion using Mn-doped Bi-Sr-vanadate was studied in the presence of H_2O_2 under condition of pseudo-first order reaction and proved that:-

(1) Mn-doped Sr-Bi-vanadate considers a surface catalytic activity towards the oxidative degradation of malathion.
(2) The active centers on the catalyst surface play an important role in H_2O_2 activation process through the formation of activated complex that stabilized by hydrogen bonding.
(3) The rate of oxidative of malathion increase with increasing concentration of malathion and H_2O_2. Also, the observation rate constant increase with increasing temperature.
(4) The rate of oxidative of malathion depends on pH and the oxidation efficiency is maximum in acidic and alkaline medium.

REFERENCES

[1] C.Carvalho, A.Fernandes, A.Lopes, H.Pinheiro, I.Goncalves; Chemosphere, **67(7)**, 1316-1324 **(2007)**.
[2] A.R.Dincer, Y.Günes, N.Karakaya; J.Hazard. Mater., **141(3)**, 529-535 **(2007)**.
[3] Y.Ku, K.Y.Chen, K.C.Lee; Water Res., **31(4)**, 929-935 **(1997)**.
[4] M.Lapertot, S.Ebrahimi, S.Dazio, A.Rubinelli, C.Pulgarin; J.Photochem.Photobiol.A, **186(1)**, 34-40 **(2007)**.
[5] S.Irmak, E.Kusvuran, O.Erbatur; Appl.Catal.B, **54(2)**, 85-91 **(2004)**.
[6] Sh.Song, H.P.Ying, P.Zh.He, J.M.Chen; Chemosphere, **66(9)**, 1782-1788 **(2007)**.
[7] B.Zh.Guo, H.Ch.Gu, Zh.Zheng, R.Feng, F.Jiang, G.Zh.Gao, Y.F.Zheng; Ultrason.Sonochem., **13(6)**, 487-492 **(2006)**.
[8] Agrochemicl hand book, **(1988)**.
[9] Jun Wang, Zhijun Pan, Zhaohong Zhang, Xiangdong Zhang, Yuefeng Jiang, Teng Ma, Fuyu Wen, Ying Li, Peng Zhang; Dyes and Pigments, **74(3)**, 525-530 **(2007)**.
[10] M.H.Robbins, R.S.Drago; J.Catalysis, **170**, 295 **(1997)**.
[11] N.Greenwood, A.Earshaw; Chemistry of the Elements, Pregmon New York, USA, **(1989)**.
[12] R.S.Drago, R.H.Beer; Inorg.Chem.Acta., **198**, 359 **(1992)**.
[13] U.Nickel, B.Klein, Ber.Bunsenges; Phys.Chem., **91**, 997 **(1991)**.
[14] M.Khaled Elsabawy, M.A.Morsy Sekkinna, A.Hosny El-Daly, M.Jansen; Inorganic Chemistry: Indian J., **2**, 1 **(2007)**.
[15] P.C.Pavan, E.L.Crepaldi, G.D.A.Gomes, J.B.Valim; Colloids; Surfaces A, **154**, 399 **(1999)**.
[16] Y.Cao, J.Chen, L.Huang, Y.Wang, Y.Hou, Y.Lu; Journal of Molecular Catalysis A, Chemical, **233(1-2)**, 24 May,p 61-66 **(2005)**.
[17] S.Kaneco, M.A.Rahman, T.Suzuki, H.Katsumata, K.Ohta; J.of Photochem.and Photobiology A: Chemistry, **163(3)**, 419-424 **(2004)**.
[18] C.B.Maugans, A.Akgerman; Water Research, **31(12)**, 3116-3124 **(1997)**.
[19] J.J.Delgado, J.A.Pérez-Omil, J.M.Rodríguez-Izquierdo, M.A.Cauqui; Catalysis Communications, **7(9)**, 639-643 **(2006)**.
[20] U.R.Pillai, S.Deevi; Appl.Catal.B: Environ., **64**, 146 **(2006)**.
[21] J.Bandara, J.Kiwi, C.Pulgarin, P.Peringer, G.M.Pajonk, A.Elaloui, P.Albers; Environ.Sci. Technol., **30**, 1261 **(1996)**.
[22] J.Bandara, I.Guasaquillo, P.Bowen, L.Soare, W.F.Jardim, J.Kiwi; Langmuir, **21**, 8554 **(2005)**.
[23] M.Paschoalino, N.C.Guedes, W.Jardim, E.Mielczarski, J.A.Mielczarski, P.Bowen, J.Kiwi; J.Photochem.Photobiol.A: Chem., **199**, 105 **(2008)**.

[24] H.Fan, L.Yang, W.Hua, X.Wu, Z.Wu, S.Xie, B.Zou; Nanotechnology, **15**, 37 **(2004)**.

[25] C.F.Smith, W.H.McCurdy; Anal.Chem., **24**, 372 **(1952)**.

[26] M.M.Halmann; Photodegradation of Water Pollutants, CRC Press, **(1995)**.

[27] J.K.Kim, F.Martinez, I.S.Metcalfe; Catal.Today, **124**, 224 **(2007)**.

[28] G.R.Helz, R.G.Zepp, D.G.Crosby; Aquatic and Surface Photochemistry, Lewis Publishers, **(1994)**.

[29] D.D.Dionysiou, M.T.Suidan, E.Bekou, I.Baudin, J.M.Laine; Appl.Catal.B: Environ., **26**, 153 **(2000)**.

[30] D.D.Dionysiou, M.T.Suidan, E.Bekou, I.Baudin, J.M.Laine; Appl.Catal.B: Environ., **50**, 259 **(2004)**.

[31] C.Shifu, L.Yunzhang; Chemosphere, **67**, 1010 **(2007)**.